# Image Segmentation Using Morphological Filters and Region Merging

N. Santhi and K. Ramar

Department of ECE, N.I. College of Engineering, Kumaracoil, Tamilnadu, India

Department of IT, National Engineering College, Kovilpatti, Tamilnadu, India

**Abstract:** Automatic image segmentation is one of the most Challenging problems in computer vision. This study presents a novel algorithm to partition an image with low Depth-of-Field (DOF) into focused Object-of-Interest (OOI) and defocused background. The proposed algorithm unfolds into three steps. In the first step, we transform the low-DOF image into an appropriate feature space, in which the spatial distribution of the high-frequency components is represented. This is conducted by computing Higher Order Statistics (HOS) for all pixels in the low-DOF image. Next, the obtained feature space, which is called HOS map in this study, is simplified by removing small dark holes and bright patches using a morphological filter by reconstruction. Finally, the OOI is extracted by applying region merging to the simplified image and by thresholding. Unlike the previous methods that rely on sharp details of OOI only, the proposed algorithm complements the limitation of them by using morphological filters, which also allows perfect preservation of the contour information.

**Key words:** Segmentation, mosphological filters, algorithm, DOF, HOS

## INTRODUCTION

The objective of image segmentation is to partition an image into homogeneous Regions. In this study, we describe a novel segmentation Algorithm for images with low Depth-of-Field (DOF). Low DOF is an important photographic technique commonly Used to assist viewers in understanding the depth information within a two-dimensional (2-D) photograph. Unlike typical Image segmentation methods (Basl and Jain, 1988; Hifshitz and Pizer, 1990; Comaniciu and Meer, 1997) in which regions are discovered using properties of the intensity or texture, focus, cue may play the most important role for the automatic extraction of the focused OOI. The fact that we can extract a semantically Meaningful object automatically from low-DOF images Suggests a variety of applications, such as image indexing For content-based retrieval, object-based image compression, Video object extraction, three-dimensional (3-D) microscopic Image analysis, image enhancement for digital camera, range Segmentation for depth estimation and fusion of multiple images, Which are differently focused.

There are two approaches to the segmentation of the low-DOF images: Edge-based and region-based approaches. The edge-based method extracts the boundary of the object by measuring the amount of defocus at each edge pixel. The algorithm has demonstrated high accuracy for segmenting man-made objects and objects with clear boundary edges. However, this approach often fails to detect boundary edges of the natural object, yielding disconnected boundaries. The region-based segmentation algorithms rely on the detection of the high frequency areas in the image. A reasonable starting point is to measure the degree of focus for each pixel by computing high-frequency components. To this end, several methods have been used, such as spatial Summation of the Squared Anti-Gaussian (SSAG) function, variance of wavelet coefficients in the high-frequency bands, a multiscale statistical description of high-frequency wavelet coefficients, local variance and so on. Note that exploiting high-frequency components alone often results in errors in both focused and defocused regions. In defocused regions, despite blurring due to defocusing, there could be busy texture regions in which high-frequency components are still strong enough. These regions are prone to be misclassified as focused regions. Conversely, we may have focused regions with nearly constant gray levels, which also generate errors in these regions.

In this study, we consider an efficient and fast segmentation Algorithm to compute Higher Order Statistics (HOS) for each pixel, which effectively assesses the amount of high-frequency components in the focused regions, whereas less sensitive to noises in the defocused regions. Then, we employ a morphological approach so that even focused smooth areas can be merged into the

surrounding areas with high-frequency components (i.e., edges). The final decision of the focused regions is conducted by region merging and thresholding.

## DEPTH OF FIELD AND LOW DOF

The depth of field is the range of distances over which objects are focused "sufficiently well," in the sense that the diameter of the blur circle is less than the resolution of the imaging device. The DOF depends, of course, on what sensor is used, but in any case it is clear that the larger the lens aperture, the less the DOF. Clearly, errors in focusing become more serious when a large aperture is employed. As shown in Fig. 1 and are the front and rear limits of the "depth of field." With low DOF, only the OOI is in sharp focus, whereas objects in background are blurred to out of focus. Photographers often use this photographic technique to point their interest in the image or to help viewers understand the depth information from the 2-D image. Examples are shown in Fig. 1.

## PROPOSED ALGORITHM

Let R represent a set of pixels, $R = \{(x, y); 1 \le x \le X, 1 \le y \le Y\}$ where the image size is $X \times Y$. Our goal is to partition R into sharply focused objects-of-interest, denoted by OOI and remaining regions, expressed by $\overline{OOI}$. Let $P = \{R_i, i \in \{1, \ldots, N\}$ denote a partition of R. The OOI of an image is defined as follows:

$$OOI = \bigcup_{i=1}^{NOOr} R_i$$

Where $R_i$ is the connected region and $N_{OOI}$ denotes the number of regions belonging to OOI. In other words, OOI represents the focused objects of interest, composed of regions of $N_{OOI}$.

**Feature space transformation using HOS:** The first step toward segmentation consists in transforming the input low-DOF image into an appropriate feature space. The choice of the feature space depends on the applications that the algorithm is aimed at. For instance, the feature space may represent the set of wavelet coefficients (Wang *et al.*, 2001) or local variance image field (Won *et al.*, 2002).

In our case, we compute HOS for feature space transformation. HOS are well suited to solving detection and classification problems because they can suppress Gaussian noise and preserve some of the non-Gaussian information (Gelle *et al.*, 1997; Tsatsanis and Giannakis, 1992). At a pixel $(x,y) \in R$, a component of the HOS map, HOS(x,y), is defined as follows.



Fig. 1: Low DOF image

$$HOS(x,y) = \min\left(255, \frac{\overline{m}^{(4)}(x,y)}{DSF}\right)$$

Where DSF denotes down scaling factor. For a variety of test images, it is observed that 100 is appropriate for DSF. Hence, DSF has been set to 100 throughout the study. HOS map yields denser and higher values in the focused areas, suppressing noise in the defocused regions.

**HOS map simplification by morphological filtering and boundary detection by snake algorithm:** The HOS map transformed from the low-DOF image has gray levels ranging from 0 to 255, where high values indicate the existence of high-frequency components (i.e., possibly focused regions). However, as mentioned earlier, there could be some focused smooth regions, which may not be easily detected by HOS transformation. Similarly, defocused texture regions may generate noise. Therefore, a proper tool for HOS map simplification is needed to remove these errors, appearing in the form of small dark and bright patches in focused and defocused regions, respectively.

Morphological filtering is well known as a useful approach to smooth noisy gray-level images by a determined composition of opening and closing with a given structuring element. A large number of morphological tools rely on two basic sets of transformations known as erosion and dilation. Let B denote a window or flat structuring element and let $B_{x,y}$ be the translation of B so that its origin is located at $(x,y) \in R$. Then, the erosion $\varepsilon_B(O)$ of a HOS map O by the structuring element B is used in constructing a morphological filter for image simplification $\varepsilon_B(O)(x,y) = \min_{(k,l) \in B_{x,y}} HOS(k,l)$. Similarly, the dilation $\delta_B(O)(x,y) = \max_{(k,l) \in B_{x,y}} HOS(k,l)$. Elementary erosions and dilations allow the definition of morphological filters such as morphological opening and closing: Morphological opening $\gamma_B(O)$ and closing $\varphi_B(O)$, are given by $\gamma_B(O) = \delta_B(\varepsilon_B(O))$ and $\varphi_B(O) = \varepsilon_B(\delta_B(O))$ respectively.

The morphological opening operator $\gamma_B(O)$ applies an erosion $\varepsilon_B()$ followed by a dilation $\delta_B()$. Erosion leads to darker images, where as dilation to brighter images.

275

A morphological opening (resp. closing) simplifies the original signal by removing the bright (resp. dark) components that do not fit within the structuring element B . This morphological operators can also be directly applied to binary image without any modification.

The disadvantage of these operators is that they do not allow a perfect preservation of the contour information. To overcome this problem, so-called filters by reconstruction are preferred Although similar in nature, they rely on different erosion and dilation operators, making their definitions slightly more complicated. The elementary geodesic erosion $\varepsilon^{(1)}(O,O_R)$ of size one of the original image O with respect to the reference image $O_R$ is defined as $\varepsilon^{(1)}(O,O_R)(x,y)=\max\{\varepsilon_B(O)(x,y),O_R(x,y)\}$ and the geodesic dilation $\delta^{(1)}(O,O_R)$ of size one of the original image O with respect to the reference image $O_R$ is defined as:

$$\delta^{(1)}(O,O_R)(x,y)=\min\{\delta_B(O)(x,y),O_R(x,y)\}$$

Thus, the geodesic dilation $\delta^{(1)}(O,O_R)$ dilates the image O using the classical dilation operator $\delta_B(O)$ . As we know, dilated gray values are greater or equal to the original values in O. However, geodesic dilation limits these to the corresponding gray values of $O_R$ . The choice of the reference image will be discussed shortly.

Geodesic erosions and dilations of arbitrary size are obtained by iterating the elementary versions $\varepsilon^{(1)}(O,O_R)$ and $\delta^{(1)}(O,O_R)$ accordingly. For example, the geodesic erosion (dilation) of infinite size, which is so-called reconstruction by erosion (by dilation) is given by the following.

- Reconstruction by erosion:

$$\varphi^{(rec)}(0,0_R)=\varepsilon^{(\infty)}(0,0_R)=\varepsilon^{(1)}=\varepsilon^{(1)}0\varepsilon^{(1)}o...o\varepsilon^{(1)}(0,0_R)$$

- Reconstruction by dilation:

$$\gamma^{(rec)}(0,0_R)=\delta^{(\infty)}(0,0_R)=\delta^{(1)}=\delta^{(1)}0\delta^{(1)}o...o\delta^{(1)}(0,0_R)$$

Notice that $f^{(rec)}(O,O_R)$ and $\gamma^{(rec)}(O,O_R)$ will reach stability after a certain number of iterations.

In the proposed system, we employ morphological closing-opening by reconstruction, which is morphological closing by reconstruction followed by morphological opening by reconstruction. The strength of the morphological closing-opening by reconstruction filter is that it fills small dark holes and removes small bright isolated patches, whereas perfectly preserving other components and their contours. Obviously, the size of removed components depends on the size of the structuring element.
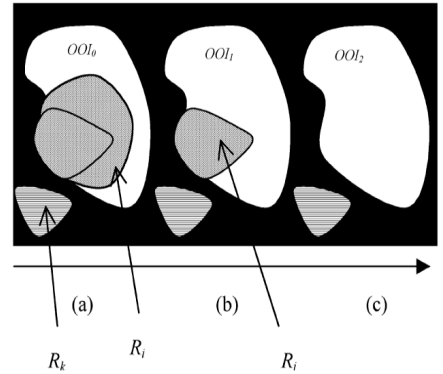


Fig. 2: Evolution of OOI (a) initial OOI (b) $R_i$ merged into OOI (c) final OOI

**Region merging and adaptive thresholding:** In typical morphological segmentation techniques, the simplification by morphological filters is followed by marker extraction and watershed algorithm to partition an image or scene into homogeneous regions in terms of intensity. The marker extraction step selects initial regions, for instance, by identifying large regions of constant gray level obtained in the simplification step. After the marker extraction, the number and the interior of the regions to be segmented are known.

However, a large number of pixels are not yet assigned to any region. These pixels correspond to uncertainty areas mainly concentrated around the contours of the regions. Assigning these pixels to a given region can be viewed as a decision process that precisely defines the partition. The classical morphological decision tool is the watershed, which labels pixels in a similar fashion to region growing techniques.

Unlike the above mentioned conventional intensity-based segmentation schemes, the task of the low-DOF image segmentation is to extract focused region (i.e., OOI) from the image rather than partitioning the image. In this case, the reasonable way is to grow initially detected focused regions until they occupy all the focused regions. In the following, we propose a decision process, which is composed of two steps: region merging and final decision by thresholding.

**Region merging:** Our region merging is started based on seed regions, which can be regarded as definitely focused regions of OOI. First, every flat zone is treated as a region regardless of its size, which means even one pixel zone can become a region. Then, we define regions having the highest value in the simplified HOS map as seed regions and these seed regions become initial OOI [see white areas in Fig. 2(c) and (a)]. We also define regions having values less than or equal to a predefined value $T_L$ $(T_L<v_h)$

as definitely defocused regions. Those regions are labeled as initial OOI$^c$. Then, the remaining regions are labeled as uncertainty regions with pixel values ($T_L, v_h$). A pictorial example is shown in Fig. 2(a), where the initial OOI and OOI are denoted by white and black regions, respectively, whereas the dashed regions $R_i$, Rj and $R_k$ indicate uncertainty regions. Our goal in this region merging process is to assign uncertainty regions to either OOI or OOI$^c$. Such an assignment is iteratively conducted by considering bordering relationship between uncertainty region and current OOI and OOI$_n$ (i.e., OOI at the iteration). Specifically, we develop an algorithm that assigns an i$^{th}$ uncertainty region $R_{n,i}$ in the n$^{th}$ iteration to either OOI or OOI$_n^c$ by computing normalized overlapped boundary (nob).

**Final decision:** In the preceding subsection, the focused regions (i.e., OOI) are updated by region merging. Now, the final decision becomes to extract OOI from the final partition P. It is easily done by extracting regions having the highest value. For instance, in Fig. 2(c), OOI will be extracted whereas $R_k$ will not be decided as OOI since it has a value than less than that of OOI.

## EXPERIMENTAL RESULTS

The proposed algorithm has been implemented and tested on low-DOF images selected from the JPEG compressed COREL CD-ROM image collection. Color images are first transformed into gray level images in our system. We used a neighborhood of size 3×3 for ç. The threshold value to determine the initial OOI was set to be 20 in the tests. One of the most important parameters is the size of the Structuring Element (SE) of the morphological filter.

We used rectangular SE and set the size to be 31×31 for all experiments except the image shown in Fig. 2(a). Since the size of the ball shown in the figure is too small, it is removed by the filter when 31×31 of SE is used. For a bettersubjective result, 21×21 of SE was employed on this image only. Figure 3 gives some experimental results of the proposed algorithm. It shows outcomes of each process for several test images. The proposed algorithm yields more accurate results over various images with low DOF.
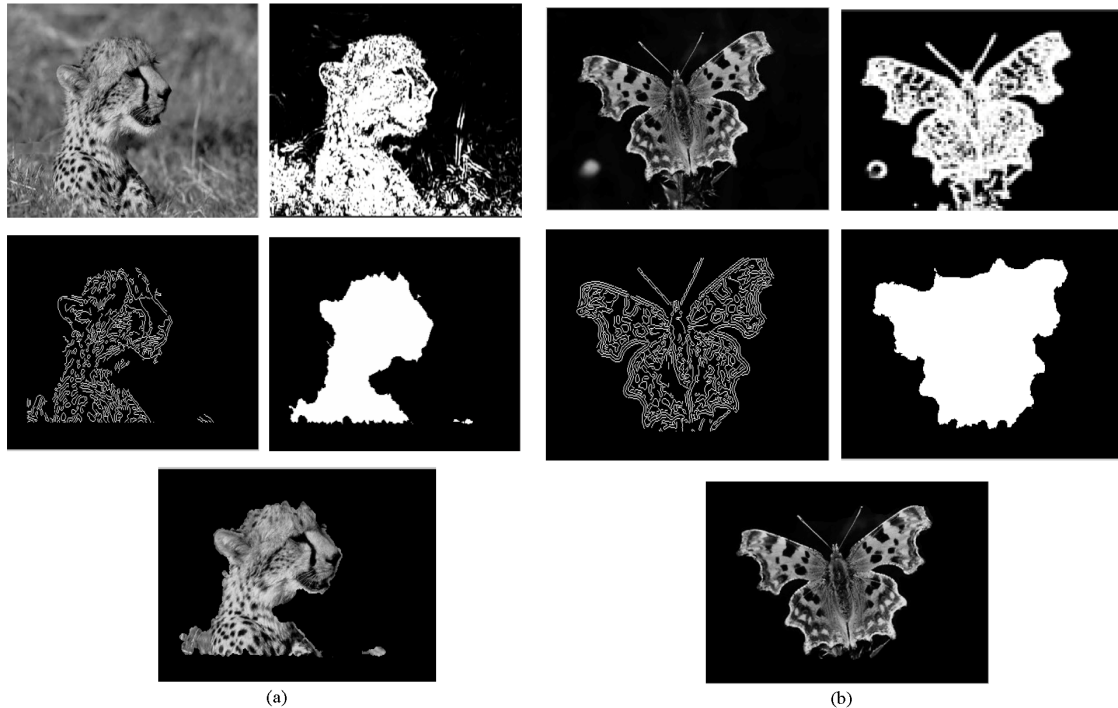


(a)             (b)

Fig. 3: Experimental results from each process.(a) Original image (b) HOS map (c) Simplified and boundary detected image (d) Region merging (e) Final decision by thresholding
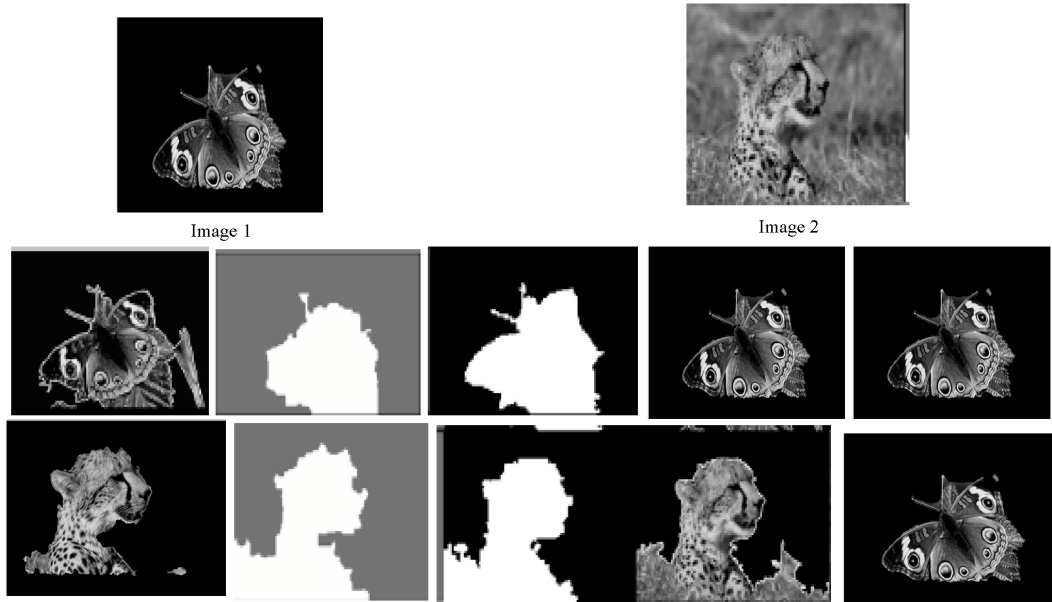
Fig. 4: Visual comparison of segmentation results. (a) Low-DOF images. (b) Results from (Wang *et al.*, 2001). (c) Results from (Yimand and Bovik, 1998). (d) Results from (Ye and Lu, 2002). (e) Results from the proposed algorithm

Table 1: Shows the spatial distortion measures of the results from

| Image | Ref[2] | Ref[8] | Ref[9] | Proposed |
|-------|--------|--------|--------|----------|
| 1 | 0.13 | 0.05 | 0.16 | 0.04 |
| 2 | 0.29 | 0.26 | 0.44 | 0.10 |

The morphological filter approach in this research very promising and yields more accurate results over various images with low DOF Future works can be done using different filters to get reasonable results .The performance of the proposed algorithm is also evaluated by using objective criterion. In (Wang *et al.*, 2001) the performance is evaluated by sensitivity, specificity and error rate. However, since they are defined as the ratios of the areas, even different shape of areas can show high performance as far as the size of the extracted OOI (or background) is close to that of reference. We propose to use a pixel-based quality measure which was used to evaluate the performances of video object segmentation algorithms (Fig. 4).

The spatial distortion of the estimated OOI from the reference OOI is defined as:

$$d(O^{est}, O^{ref}) = \frac{\sum_{(x,y)} O^{est}(x,y) \otimes O^{ref}(x,y)}{\sum_{(x,y)} O^{ref}(x,y)}$$

where $O^{est}$ and $O^{ref}$ are the estimated and reference binary masks, respectively. Table 1 shows the spatial distortion measures of the results from (Wang *et al.*, 2001); Ye and Lu, 2002; Gella *et al.*, 1997).

**CONCLUSION**

We developed an algorithm that separates the pixels in the low-DOF images into two regions based on their higher order statistics. To this end, the low-DOF image was transformed into an appropriate feature space, which was called HOS map in this study. Morphological filter by reconstruction was applied to simplify the HOS map, followed by region-merging technique and thresholding for final decision. By employing the powerful morphological tool for simplification, the proposed scheme performs well even for focused smooth regions as far as their boundaries contain high frequency components (i.e., edges). Also, it shows its robustness to scattered sharp areas in the background thanks to the powerful morphological simplification and the following region merging. Nonetheless, if the focused smooth region is too large, the proposed algorithm may need to incorporate some semantic or human knowledge.

**REFERENCES**

Besl, P.J. and R. C. Jain, 1988. Segmentation through variable-order surface fitting, IEEE. Trans. Pattern Anal. Mach. Intell., PAMI-10, pp: 167-192.

Comaniciu, D. and P. Meer, 1997. Robust analysis of feature spaces: Color image segmentation, in Proc. IEEE Conf. Computer Vision and Pattern Recognition, San Juan, Puerto Rico, pp: 750-755.

Gonzalez, R.G. and R. E.Woods, 1992. Digital Image Processing. Reading, MA: Addison-Wesley.

Gelle, G., M. Colas and G. Delaunay, 1997. Higher order statistics for detectionand classification of faulty fanbelts using acoustical analysis, in Proc. IEEE. Signal Processing Workshop on Higher-Order Statistics, pp: 43-46.

Lifshitz L.M. and S.M. Pizer, 1990. A multiresolution hierarchical approach to image segmentation based on intensity extrema, IEEE Trans. Pattern Anal. Mach. Intell., 12: 529-540.

Tsatsanis, M.K. and G.B. Giannakis, 1992. Object and texture classification using higher order statistics, IEEE Trans. Pattern Anal. Mach. Intell., 14: 733-750.

Tsai, D.M. and H.J. Wang, 1998. Segmenting focused objects in complex visual images, Pattern Recognit. Lett., 19: 929-949.

Wang, J.Z., J. Li, R.M. Gray and G. Wiederhold, 2001. Unsupervised multiresolution segmentation for images with low depth of field, IEEE Trans. Pattern Anal. Mach. Intell., 23 : 85-90.

Won, C.S., K. Pyun and R.M. Gray, 2002. Automatic object segmentation in images with low depth of field, in Proc. Int. Conf. Image Processing, vol. III, Rochester, NY, pp: 805-808.

Yimand, C., A.C. Bovik, 1998. Multiresolution 3-D range segmentation using focused cues, IEEE. Trans. Image Process., 7: 1283-1299.

Ye, Z. and C.C. Lu, 2002. Unsupervised multiscale focused objects detection using hidden Markov tree, in Proc. Int. Conf. Computer Vision, PatternRecognition and Image Processing, Durham, NC, pp: 812-815.